Electronic Supplementary Material (ESI) for Journal of Materials Chemistry A.

$Zn:BiVO_4/Mo:BiVO_4$ Homojunction as Efficient Photoanode for Photoelectrochemical Water Splitting

Jae Myeong Lee,[a ‡] Ji Hyun Baek,[a, b ‡] Thomas Mark Gill,[b] Xinjian Shi,[b] SangMyeong Lee,[a] In Sun Cho,[c] Hyun Suk Jung,[a] and Xiaolin Zheng[b]**

*a. School of Advanced Materials Science & Engineering Sungkyunkwan University, Suwon 16419, Republic of Korea. *E-mail: hsjung1@skku.edu*
*b. Department of Mechanical Engineering Stanford University, Stanford California 94305, United States. *E-mail: xlzheng@stanford.edu*
c. Department of Materials Science & Engineering and Energy Systems Research Ajou University, Suwon 16499, Republic of Korea.
‡ These authors contributed equally to this work.

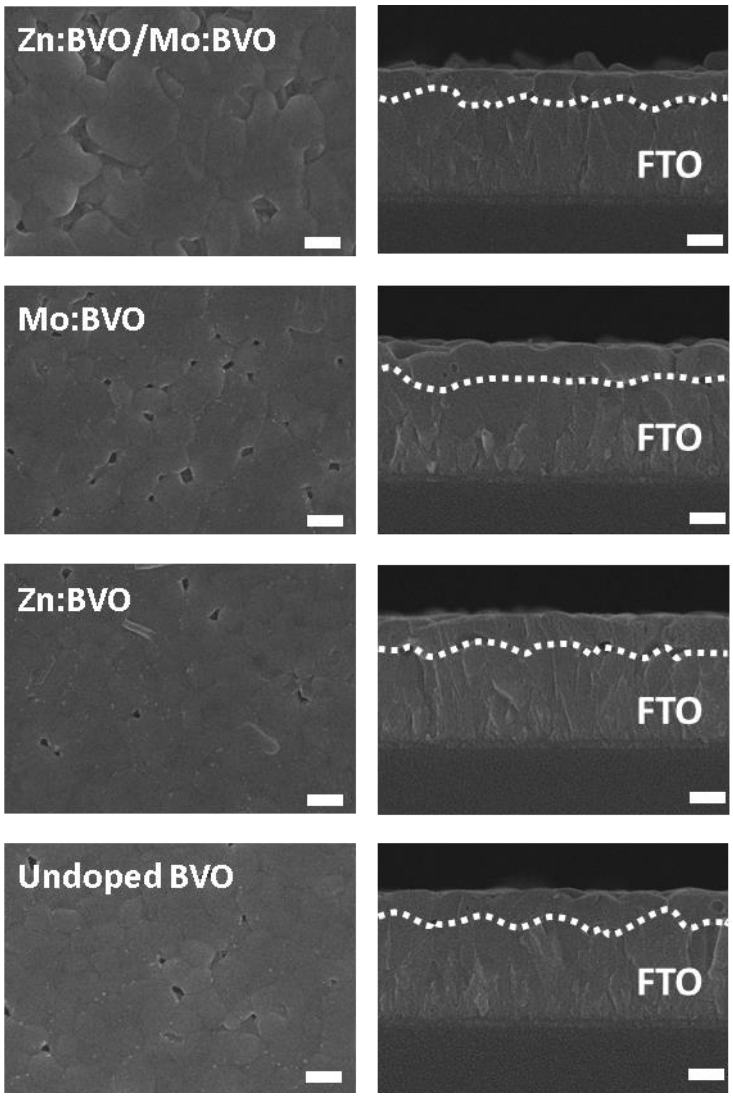

Fig. S1. SEM images of Mo:BVO, Zn:BVO and undoped BVO photoanodes. All photoanodes have similar morphologies and thickness of 300 nm (scale bar = 400 nm).

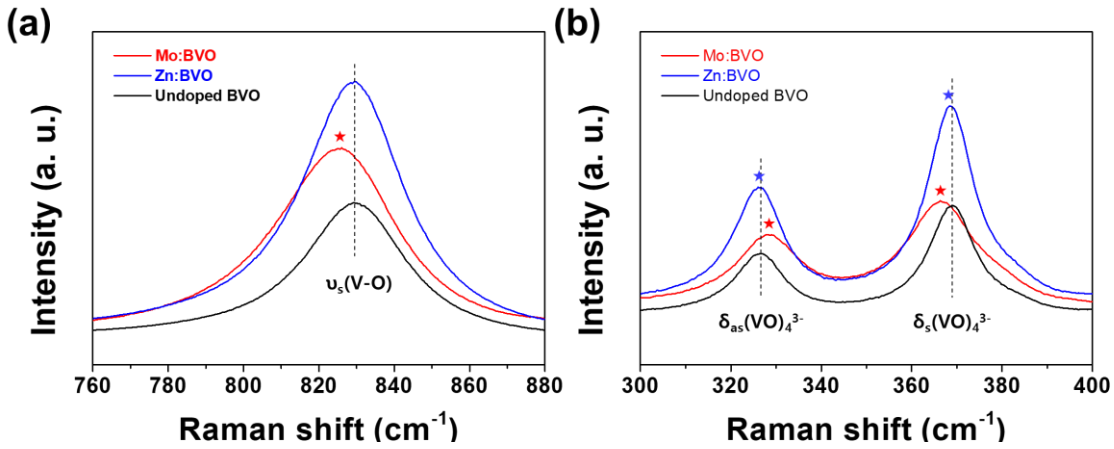

Fig. S2. Raman spectra of the (a) symmetric stretching mode and (b) symmetric and antisymmetric bending modes of Mo:BVO, Zn:BVO and undoped BVO**.**

.

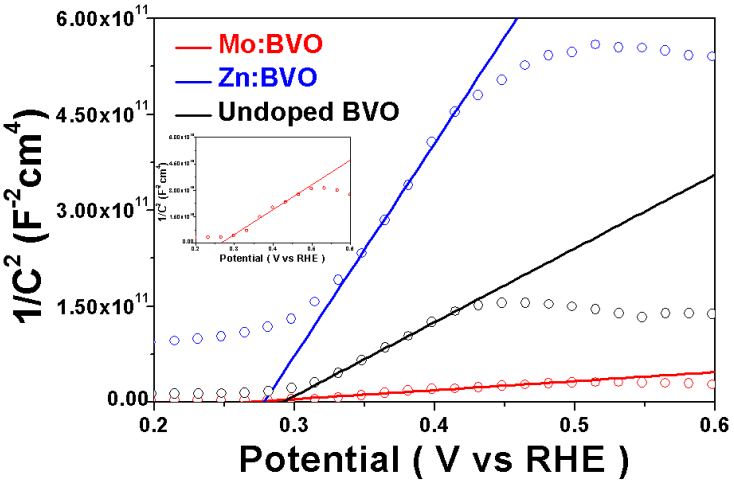

Fig. S3. Mott-schottky plots of Mo:BVO, Zn:BVO and undoped BVO photoanodes. All photoanodes indicate n-type semiconductor characteristics. The charge carrier concentrations of each photoanode were changed by doping and calculated using the following equation:[1]

$$\frac{1}{C^2} = \frac{2}{\varepsilon_0 \varepsilon_r A^2 e N_d} \left(E - E_{fb} - \frac{kT}{e}\right) \quad (1)$$

, where C is capacitance ($F^{-1}cm^2$), ε_0 is permittivity (8.85 x 10^{-14} Fcm^{-1}), ε_r is relative permittivity (68),[2] A is area (cm^2), e is elementary charge (1.602 x 10^{-19} C), N_d is donor concentration (cm^{-3}), E is applied potential (V vs. RHE), E_{fb} is flat band potential (V vs. RHE), k is Boltzmann constant (8.617 eV/K) and T is temperature (K).

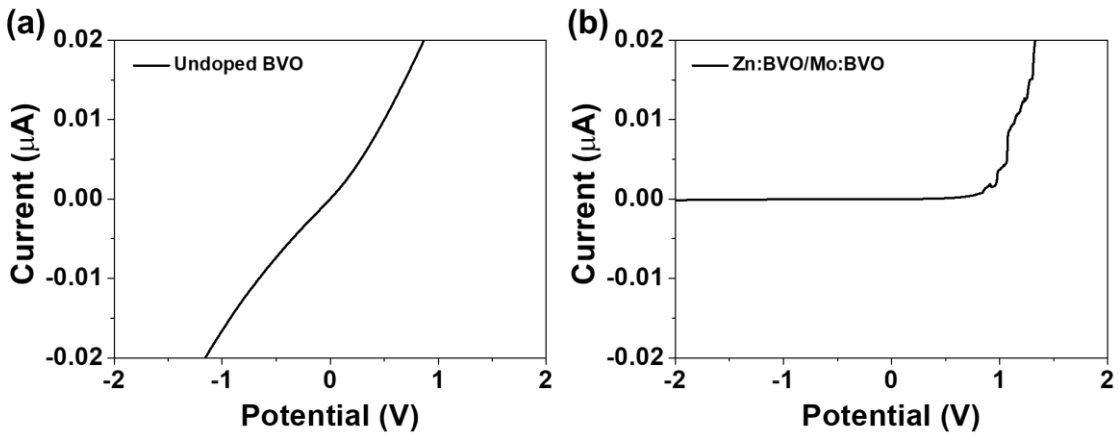

Fig. S4. I-V curves of undoped BVO and Zn:BVO/Mo:BVO homojunction photoanodes measured in air under ambient conditions. (a) The I-V characteristic of undoped BVO shows ohmic behavior and (b) that of Zn:BVO/Mo:BVO shows rectification behavior, suggesting the formation of a n-n+ junction.

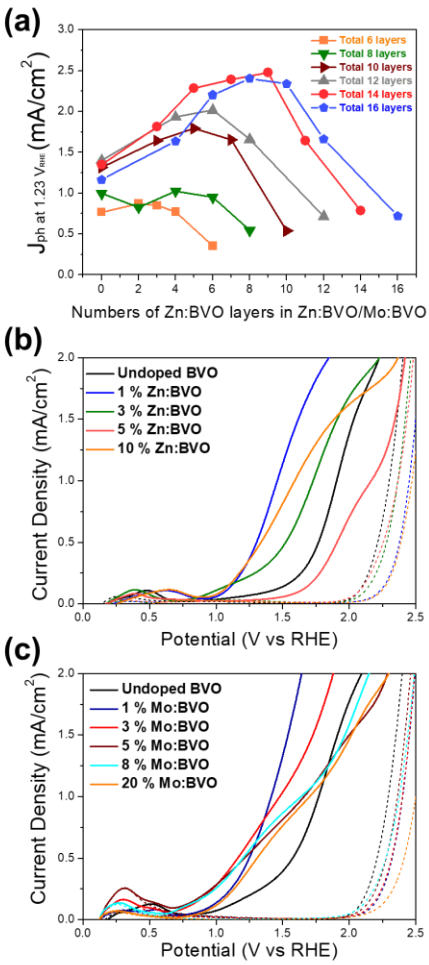

Fig. S5. (a) Thickness optimization process for Zn:BVO/Mo:BVO homojunction as we vary the total thickness and the component thickness. The thickness is quantified as numbers of spin coating layers. As a result, the junction with 9 layers of Zn:BVO and 5 layers of Mo:BVO (total 14 layers) has the best photocurrent density among all the conditions tested from total 6 to 16 layers. Dopant concentration optimization process for (b) Zn:BVO and (c) Mo:BVO, respectively. 1 % of Zn and 3 % of Mo were attained as the best condition in PEC performance at 1.23 V vs RHE.

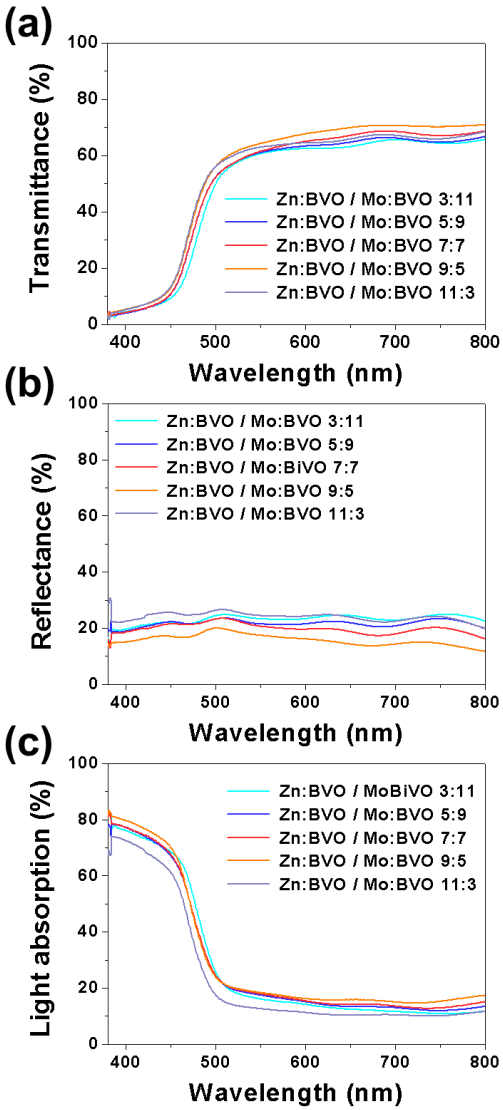

Fig. S6. Optical properties (transmittance, reflectance, and light absorption efficiencies) of 14 layers of Zn: BVO/Mo: BVO homojunction photoanode for optimization process. 9 layers of Zn:BVO and 5 layers of Mo:BVO (Zn:BVO/Mo:BVO = 9:5) has slightly better light absorption efficiency.

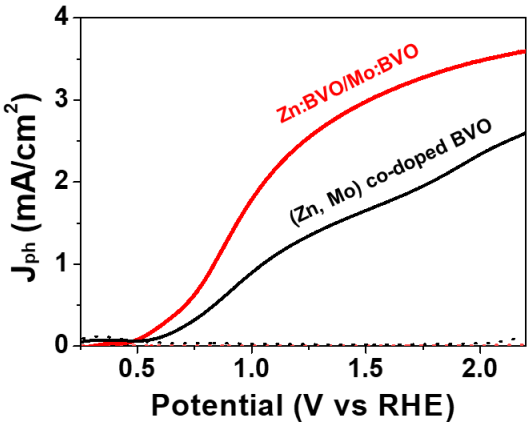

Fig. S7. J-V curves of the (Zn, Mo) co-doped BVO and Zn:BVO/Mo:BVO photoanodes under 1 sun illumination. The PEC performance of the Zn:BVO/Mo:BVO homojunction photoanode was much better than that of the (Zn, Mo) co-doped BVO photoanode.

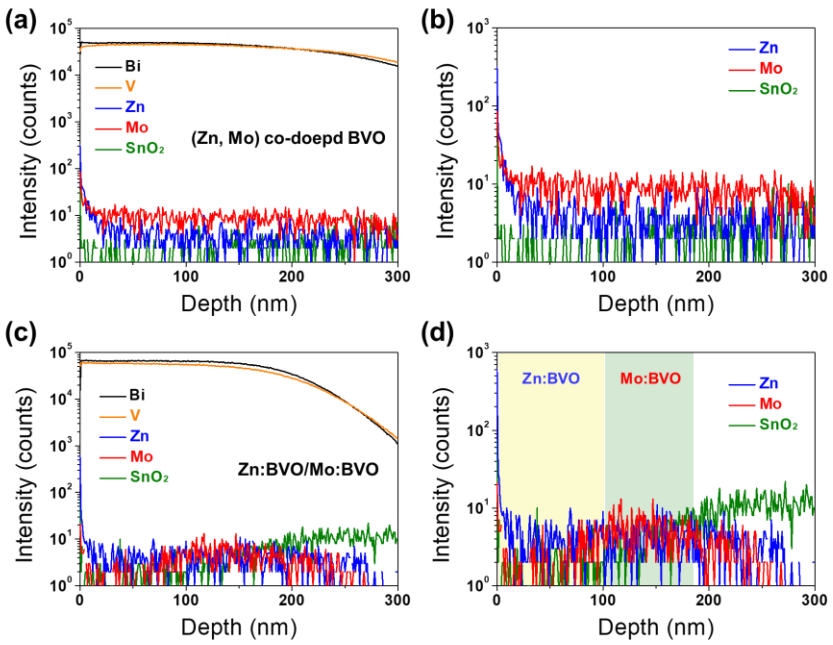

Fig. S8. Secondary ion mass spectrometry of (a) (Zn, Mo) co-doepd BVO, (b) magnified plot from (a), (c) Zn:BVO/Mo:BVO homojunction photoanode and (d) magnified plot from (c).

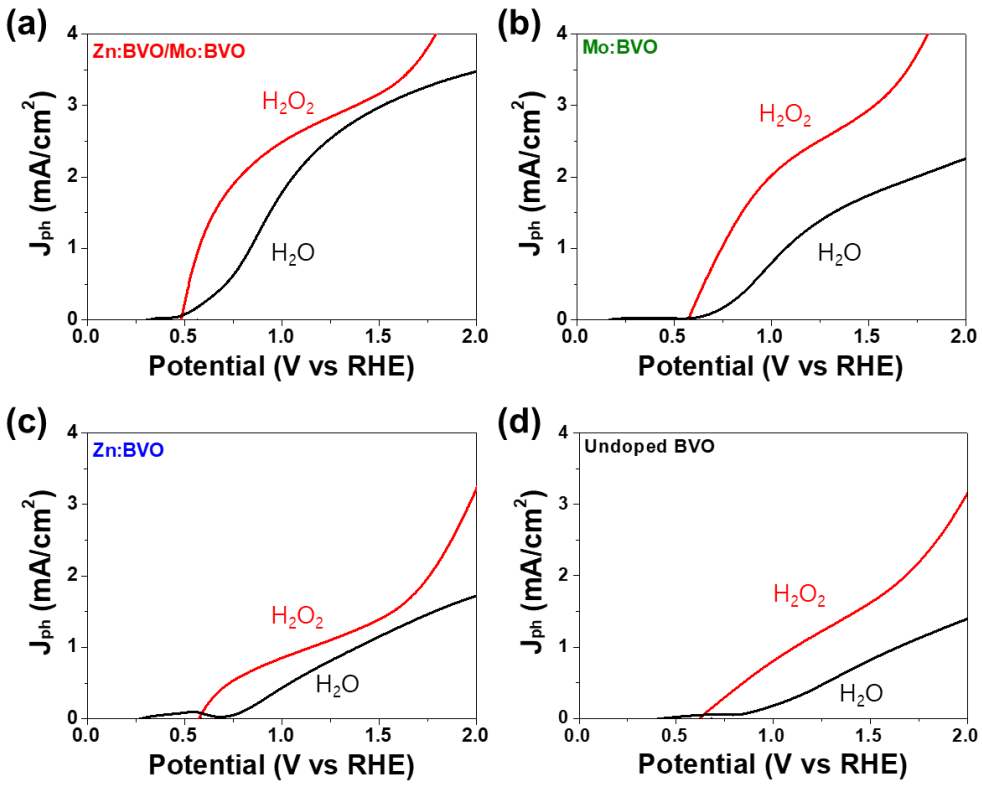

Fig. S9. J-V curves of (a) Zn:BVO/Mo:BVO homojunction, (b) Mo:BVO, (c) Zn:BVO and (d) undoped BVO photoanodes with H_2O_2. Photocurrent density measured in the electrolyte with H_2O_2 can be assumed as all holes generated are used for water oxidation. The charge transfer and bulk transport efficiencies of four photoanodes were evaluated using the H_2O_2 hole scavenger method.[3] The relationships between current density, light absorption, transfer efficiency and transport efficiency are as follows:

$$J_{Ph} = J_{abs} \times \eta_{tranfer} \times \eta_{transport} \quad (2)$$

$$\eta_{tranfer} = \frac{J_{H_2O}}{J_{H_2O_2}} \quad (3)$$

$$\eta_{tranport} = \frac{J_{H_2O_2}}{J_{abs}} \quad (4)$$

, where $\boldsymbol{J_{Ph}}$ is the measured photocurrent density, $\boldsymbol{J_{abs}}$ is current density calculated from light absorption, $\boldsymbol{\eta_{tranport}}$ is the charge transport efficiency, and $\boldsymbol{\eta_{tranfer}}$ is charge transfer efficiency at the interface between the surface and electrolyte.

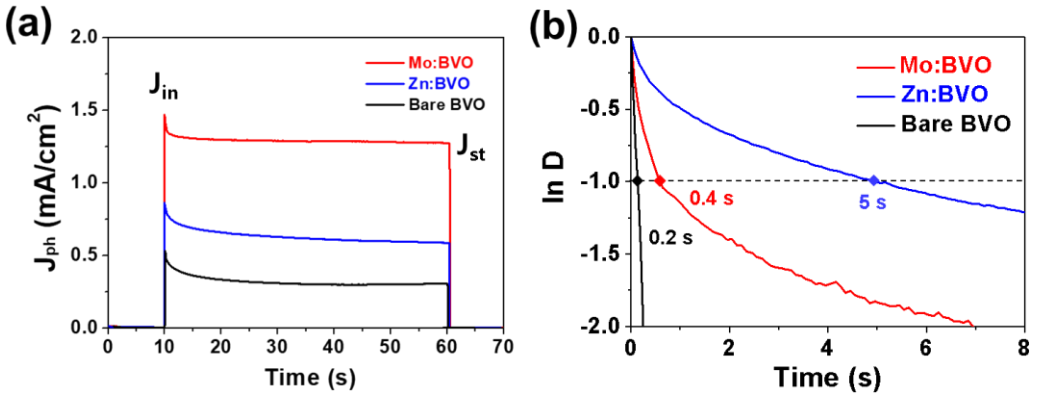

Fig. S10. (a) Transient photocurrent responses of Mo:BVO, Zn:BVO and undoped BVO photoanodes (b) Normalized plots of the current–time dependence of each photoanode at 1.23 V vs. RHE under illumination. J_{in} and J_{st} are the time-dependent, initial and steady-state photocurrent, respectively. Typically, the initial photocurrent, $J_{in,}$ is attributed to bulk electron-hole separation under immediate illumination, which is followed by decay to the steady state photocurrent, $J_{st,}$ due to surface charge recombination.[4] In particular, Zn:BVO took approximately 5 sec when ln D=-1 compared to Mo doped and undoped BVO (0.2 sec and 0.4 sec), suggesting dramatically improved carrier lifetimes with Zn doping.

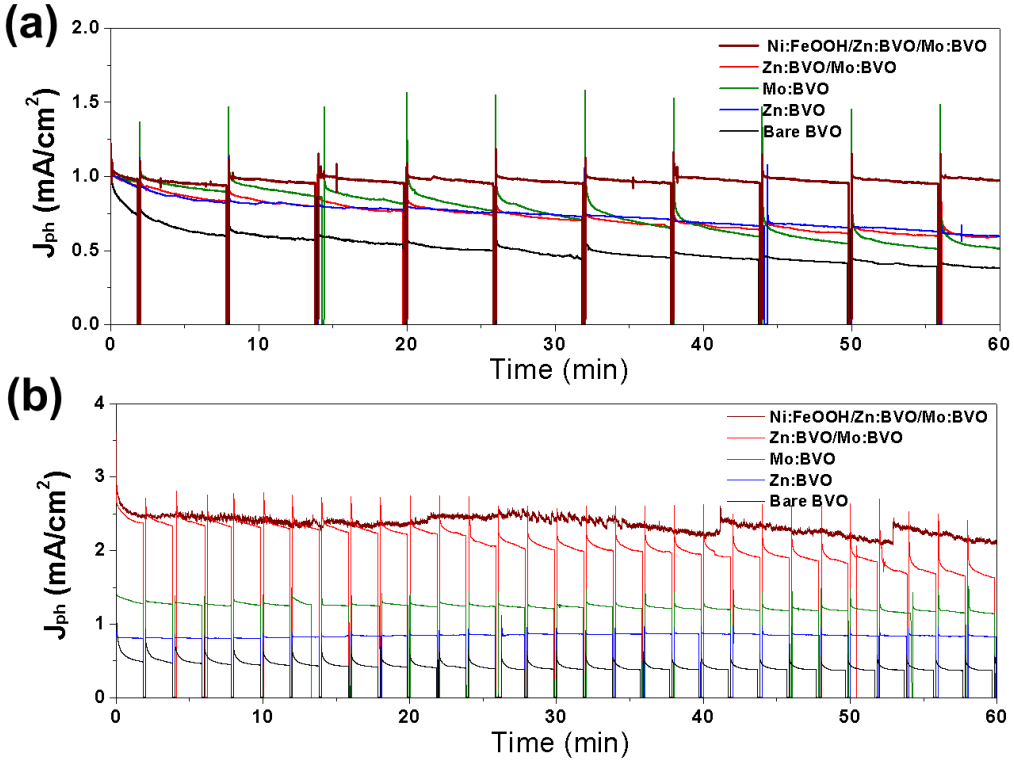

Fig. S11. Two stability tests of Ni:FeOOH/Zn:BVO/Mo:BVO, Zn:BVO/Mo:BVO, Mo:BVO, Zn:BVO, and undoped BVO photoanodes. (a) with initial current density of 1 mA/cm^2 at 0.52 V, 0.85 V, 1.12 V, 1.34 V and 1.62 V vs. RHE, respectively. (b) with same applied bias of 1.23 V vs. RHE. Conditions: the phosphate buffer solution (pH ~ 7) for 1 hour under illumination.

Table S1. Specific EIS values at each region for undoped BVO, Zn:BVO, Mo:BVO and Zn:BVO/Mo:BVO.

	R1	R2	R3
Zn:BVO/Mo:BVO	**64.80**	**123.4**	**1062**
Mo:BVO	**62.58**	**361.7**	**2742**
Zn:BVO	**64.99**	**1376**	**2389**
Undoped BVO	**61.76**	**1720**	**3601**

Table S2. Comparison of our Zn:BVO/Mo:BVO homojunction photoanode with different homojunction and heterojunction photoanodes.

	Current Density (mA/cm^2)	Thickness (nm)	Electrolyte	Process	Reference
Zn:BVO/Mo:BVO **Ni:FeOOH/Zn:BVO/Mo:BVO**	**2.5 at 1.23 V vs RHE** **2.7 at 1.23 V vs RHE**	**300**	**0.5 M Kpi (pH=7)**	**Spin coating**	**This work**
Co:BVO/Mo:BVO	**2.09 at 1.23 V RHE**	**200**	**0.1 M Kpi (pH=7)**	**Spin coating**	**Ref 5.**
Zn:BVO/BVO	**0.63 at 1.23 V vs Ag/AgCl**	**150**	**0.5 M Na2SO4**		**Ref 6.**
BVO/Mn:BVO	**2.2 at 1.24 V vs RHE**	**-**	**Na2SO4 (pH=7)**	**Spray Pyrolysis**	**Ref 7.**
BVO/TiO2	**0.8 at 1.23 V vs RHE** **2.14 at 1.7 V vs RHE**	**600**	**0.5 M Na2SO4 + Kpi (pH=7)**	**Spin coating (BVO) Hydrothermal and CBD (TiO2)**	**Ref 8.**
BVO/ZnO	**1.75 at 1 V vs RHE**	**300 (BVO)** **900 (ZnO)**	**0.2 M Na2SO4 (pH=6.5)**	**Spray pyrolysis (BVO) Hydrolysis condensation synthesis (ZnO)**	**Ref 9.**
BVO/WO3	**1.74 at 0.7 V vs Ag/AgCl**	**3000**	**0.5 M Na2SO4**	**Drop casting**	**Ref 10.**
BVO/WO3	**2.0 at 1.23 V vs RHE**	**400**	**0.1 M Kpi (pH=7)**	**Drop casting**	**Ref 11.**
BVO/SnO2	**0.95 at 1.23 V vs RHE**	**245**	**0.5 M Na2SO4 + 0.1 M Kpi (pH~7)**	**Drop casting**	**Ref 12.**

References

1. Z. Chen, H. N. Dinh and E. Miller, *Photoelectrochemical water splitting*, Springer, 2013.
2. D. Zhou, L. X. Pang, J. Guo, Z. M. Qi, T. Shao, Q. P. Wang, H. D. Xie, X. Yao and C. A. Randall, *Inorg. Chem.*, 2014, **53**, 1048-1055.
3. X. J. Shi, S. Siahrostami, G. L. Li, Y. R. Zhang, P. Chakthranont, F. Studt, T. F. Jaramillo, X. L. Zheng and J. K. Norskov, *Nat. Commun.*, 2017, **8**.
4. D. Tafalla, P. Salvador and R. Benito, *J. Electrochem. Soc.*, 1990, **137**, 1810-1815.
5. B. Zhang, H. Zhang, Z. Wang, X. Zhang, X. Qin, Y. Dai, Y. Liu, P. Wang, Y. Li and B. Huang, Appl. Catal. B-Environ., 2017, **211**, 258-265.
6. J. Z. Su, C. Liu, D. Y. Liu, M. T. Li and J. L. Zhou, Chemcatchem, 2016, **8**, 3279-3286.
7. A. Srivastav, P. Kumar, A. Verma, Y. R. Smith, V. R. Satsangi, R. Shrivastau, U. V. Waghmare and S. Dass, Int. J. Hydrogen Energy, 2018, **43**, 15815-15822.
8. B. Y. Cheng, J. S. Yang, H. W. Cho and J. J. Wu, ACS Appl Mater Interfaces, 2016, **8**, 20032-20039.
9. S. J. A. Moniz, J. Zhu and J. Tang, Adv. Energy Mater., 2014, **4**, 1301590.
10. S. J. Hong, S. Lee, J. S. Jang and J. S. Lee, Energy Environ. Sci., 2011, 4, 1781.
11. J. H. Kim, G. Magesh, H. J. Kang, M. Banu, J. H. Kim, J. Lee and J. S. Lee, Nano Energy, 2015, **15**, 153-163.
12. S. Byun, B. Kim, S. Jeon and B. Shin, J Mater Chem A, 2017, **5**, 6905-6913.